

# Optimization of Vertex Detector for International Linear Collider

Andrei Nomerotski<sup>a</sup>

<sup>a</sup>University of Oxford, Denys Wilkinson Building, Keble Road, Oxford OX1 3RH, United Kingdom

---

## Abstract

The vertex detector for the future Linear Collider needs to be as close as possible to the beampipe and to be as thin as possible. Importance of these and other parameters for the optimization is discussed together with mechanical options for thin ladders based on rigid foams.

*Key words:* vertex detector; ILC; pixel silicon detector

---

## 1. Comparison of vertex detectors

The last vertex detector of SLD, VDX3, was arguably the best vertex detector for particle physics experiments ever built (1). The detector had three layers of CCD sensors with pixels  $20 \mu\text{m} \times 20 \mu\text{m}$  around a small diameter beampipe and was very thin, 0.4% radiation length,  $X_0$  per layer. It is instructive to compare the typical impact parameter (IP) resolution of VDX3 with that of the LEP (2) and Tevatron (3) vertex detectors, all shown in Table 1. In the Table R is the radius of the first layer,  $\sigma_h$  is the single hit resolution,  $X_0$  is the radiation length per layer,  $\sigma_{IP}^{res}$  is the single hit resolution term and  $\sigma_{IP}^{ms}$  is the multiple scattering term. The resulting IP resolution for particles with momentum  $p$  passing perpendicular to the sensor can be determined using the formula:

$$\sigma_{IP} = \sqrt{(\sigma_{IP}^{res})^2 + (\sigma_{IP}^{ms}/p)^2}. \quad (1)$$

A larger beampipe for the LEP experiments is explained by the synchrotron radiation in the circular  $e^+e^-$  machine and a worse single hit resolution for

detector	R [cm]	$\sigma_h$ [ $\mu\text{m}$ ]	$X_0$ [%]	$\sigma_{IP}^{res}$ [ $\mu\text{m}$ ]	$\sigma_{IP}^{ms}$ [ $\mu\text{m}$ ]
SLD VDX3	2.8	4	0.4	8	30
SLD VDX2	2.8	5	1.2	11	70
LEP	6.3	8	1	20	65
Tevatron	2.0	8	2-3	10	40
ILC	1.5	4	0.1	4	8

the Tevatron and LEP follows from a larger pitch of the strip silicon sensors used by the experiments. The table also shows the resolution targeted for the ILC vertex detector.

The SLD IP resolution was a factor of two better than that of the LEP vertex detectors providing excellent vertexing and tracking capabilities. Comparison of the b-tagging performance for SLD and LEP experiments is shown in Figure 1. One can see that the performance of VDX3 is considerably better than for the other detectors including VDX2, the predecessor of VDX3 at SLD.

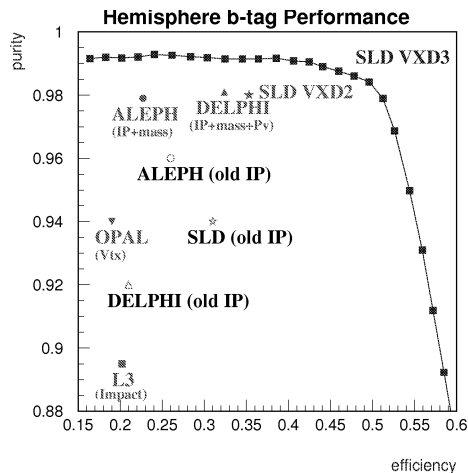


Fig. 1. Comparison of the b-tagging performance for SLD and LEP experiments.

## 2. Algorithms Based on Precise Vertexing

The superior resolution and pattern recognition of VDX3 allowed for innovative algorithms based on correct assignment of tracks to secondary and tertiary vertices. The tertiary vertices originate from the decay chains of B hadrons through D hadrons as both b- and c-quarks have considerable lifetime.

The vertex mass algorithm (4), for example, calculates the invariant mass of all tracks assigned to the secondary vertex assuming that they all are pions. This algorithm provides excellent separation between various species of quarks. This includes a good separation even between b- and c-quarks enabled by the difference in their masses. The vertex mass is the most important single contributor to the combined b-tagging procedure represented in Figure 1.

Two other important algorithms aimed to determine the sign of the quark charge are the vertex charge and vertex dipole (5). In the first one the total charge of tracks associated with a secondary vertex is calculated. Tracks from a possible tertiary vertex are included as well as they carry information about the charge of the parent. Figure 2 shows the reconstructed vertex charge for charged B mesons in Monte-Carlo simulations for ILC (6).

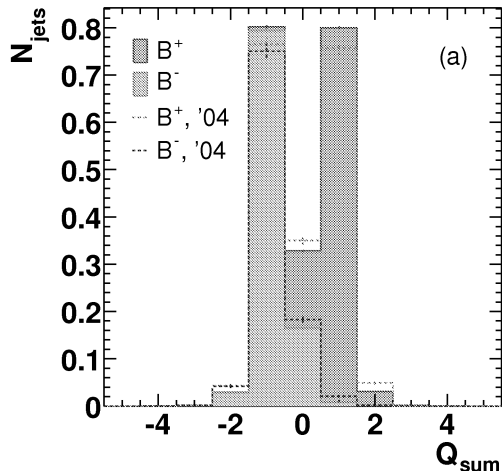


Fig. 2. Reconstructed vertex charge for  $B^+$  and  $B^-$  mesons.

The vertex charge has a binary behaviour - a lost or wrongly assigned track changes the charge of the vertex which makes every track important for the correct charge reconstruction. This particular feature makes the vertex charge algorithm sensitive to low  $p_T$  tracks hence sensitive to the amount of material as this enters the multiple scattering term in the IP resolution formula.

One of the goals of the vertex detector optimisation is comparison of different detector layouts to determine trade-offs between various design parameters. From the discussion above it is clear that the vertex charge algorithm should have a better discrimination for the designs than the b-tagging as the b-tagging relies on all tracks and contribution of a single track is averaged out.

The vertex charge algorithm is a crucial tool in a number of physics analyses. One class of such analyses includes pair production of quarks. The forward-backward asymmetry of this production in the Standard Model can be modified by various new phenomena processes (e.g. extra dimensions (8)). The full sensitivity is obtained when the asymmetry is measured as a function of the polar angle with respect to the direction of colliding particles and the flavour of the b and anti-b quarks is determined by the vertex charge. Other applications include angle correlations between heavy flavour jets and other objects in the event. This

can identify polarization of decay products of the top quarks which is also sensitive to various new physics scenarios (9). The angle correlations help to distinguish SUSY from the Little Higgs models (10) which both result in similar signatures different only in the spin of exotic neutral particles which are not detected directly. However angle correlations measured through the vertex charge of heavy quark jets are sensitive to this difference.

Another important algorithm of flavour tagging is the vertex dipole where the b or anti-b quark fragments into neutral B hadrons so it cannot be identified by the vertex charge as it is equal to zero in both cases. The vertex dipole is defined as a signed distance between secondary and tertiary vertices where the sign is defined by the difference of vertex charges in two vertices.

Other algorithms useful for optimization of the vertex detector are the bottom, charm and  $\tau$  tagging. They can be especially sensitive to the detector parameters for soft b/c/ $\tau$  jets predicted by the SUSY scenarios which are constrained by Cold Dark Matter results (10). Also a smaller lifetime of the charm quark and  $\tau$  lepton makes their identification through displaced vertices more demanding.

### 3. Dependence on Parameters

The LCFI (Linear Collider Flavour Identification) collaboration used the vertex charge as optimisation tool for initial studies of the ILC vertex detector (6). One of the most important result of the study is the sensitivity to the beampipe radius in the interaction point. Figure 3 shows the mistag rate (probability to reconstruct  $B^0$  as  $B^+$  or  $B^-$ ) as function of the jet energy for three geometries different in location of the first layer of the detector. As expected the mistag is a strong function of the minimal radius which needs to be as small as possible to obtain the best performance. To quantify the gain the corresponding luminosity factors based on the efficiency deterioration at a constant mistag have been calculated. For example, 70% more luminosity is needed for 50 GeV jets if the radius is increased from 15 mm to 25 mm assum-

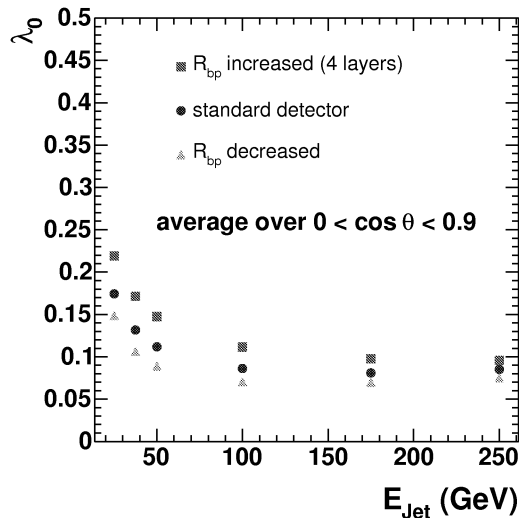


Fig. 3. Probability to reconstruct  $B^0$  as  $B^+$  or  $B^-$  as function of the jet energy for three geometries different in location of the first layer of the detector.

ing double-tagging of b-jets. Note that the increase will also require the increase of the thickness for the Be beampipe from 0.4 mm to 1 mm (6).

Figure 4 shows the effect of various parameters on the mistag rate. The default configuration (minimal radius 15 mm,  $P_T$  cutoff in tracking 0.1 GeV and thickness per layer 0.1%  $X_0$ ) is compared to configurations where one of these three parameters has been changed (minimal radius 25 mm,  $P_T$  cutoff in tracking 0.2 GeV and thickness per layer 0.4%  $X_0$ ). Strong sensitivity to material and  $p_T$  cutoff has been observed. Note that in these studies the ideal tracking (no fake tracks) has been used and no secondaries from interactions with material have been assumed so the real performance is expected to be somewhat worse. Apart from the multiple scattering term in IP resolution there are some additional material effects that are worth mentioning - production of the secondaries and also tails in the resolution function. The gamma conversions and generation of energetic delta-electrons in the material of the detector will increase the overall occupancy and will create displaced vertices in the vertex detector volume. Their effect will depend on the sophistication of the reconstruction software so its evaluation will require full simulation of the detector and a realistic tracking and vertexing code.

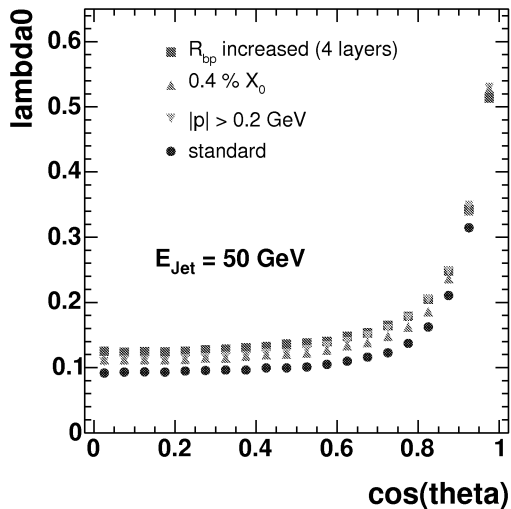


Fig. 4. Degradation in performance for minimal radius 25 mm,  $P_T$  cutoff in tracking 0.2 GeV and thickness per layer 0.4%  $X_0$ .

Another important topic in the discussion of material balance in the vertex detector is the inhomogeneity of the material distribution which will result in the tails of the resolution function. This can be accounted for by accurate description of material in the reconstruction software. The tails of the resolution can also originate from several other reasons like the angle and  $p_T$  dependence of the resolution or the clustering algorithm. Accurate description of material and sophistication of the reconstruction software are important to take advantage of a good detector.

To fully explore the sensitivity of various designs to the mentioned above parameters one needs a suite of software tools which should include realistic simulations of interactions with the detector material and advanced tracking and vertexing packages. One of them, the vertexing package ZVTOP developed by the LCFI collaboration, includes the topological vertex finder ZVTOP, additional ghost track enhancement algorithm ZVKIN and is fully integrated into the ILC MonteCarlo, tracking and software frameworks. The package has been inspired by the vertexing code used by the SLD detector (7). The package also has a flavour tagging part based on a neural net algorithm.

Considerations above show that the thinnest

possible detector is needed but, of course, the final design will be a trade-off between the ideal and reality. The TESLA TDR released in 2001 had the thickness of the vertex detector at 0.06%  $X_0$  per layer. This has been changed in 2003 to a more realistic number 0.1% and stayed at this number till now. All effort should be made to maintain this goal as this is a crucial parameter.

The above considerations were to demonstrate that the Linear Collider conditions allow to do much more sophisticated vertexing algorithms than at other machines through the correct particle assignment to secondary and tertiary vertices. The two big items in the vertex detector optimization are the small diameter beampipe and the thin detector. Next section discusses how to achieve the 0.1% radiation length per layer.

#### 4. Mechanical Options

The target of 0.1%  $X_0$  per layer which is equivalent to 100  $\mu\text{m}$  of silicon is a huge challenge. Studies carried out during the last years by the LCFI collaboration already investigated several methods. Unsupported thin silicon where the longitudinal tensioning provides stiffness has no lateral stability and is not believed to be promising. The other technique involved thin substrates of various materials. In this case a silicon sensor is thinned to the epitaxial layer of about 25  $\mu\text{m}$  and then glued to a low mass substrate which provides lateral stability. The longitudinal stiffness in this case is still coming from a moderate tension. Beryllium has the best specific stiffness and has been used before at SLD where the ladder was composed of 0.15 mm of Si and 0.37 mm of Be.

Ladders based on Be and carbon fibre (CF) substrates have been constructed with the total thickness of 0.15%  $X_0$  achieved for Be and 0.09% for CF. The CTE mismatch was causing a rippling effect for Be while for the CF substrate the mismatch is much smaller and the rippling does not occur. However in both cases the lateral stability was determined to be insufficient.

The most promising technique investigated so far is based on rigid foam structures made of RVC

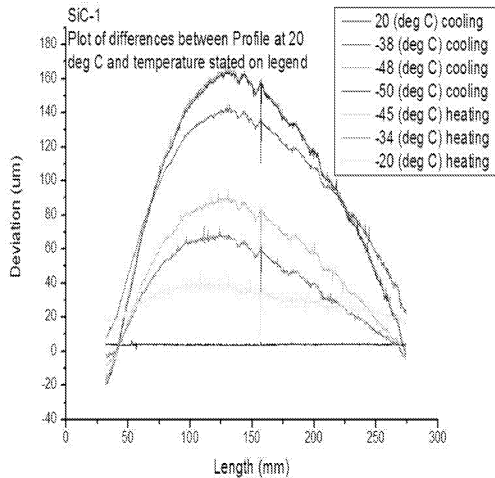


Fig. 5. Deviation from the original position as function of the location and temperature for the SiC ladder.

(Reticulated Vitreous Carbon) or SiC (Silicon Carbide) which form macroscopically uniform open cells. Several prototypes have been constructed of a 3% fill factor RVC foam sandwiched between two pieces of thin silicon and of a 8% SiC foam glued to one piece of silicon with the total thickness of 0.09% and 0.14%  $X_0$  correspondingly. The first structure has been determined to be mechanically unsatisfactory while the second one performed well. Figure 5 shows deviation from the original position as function of the location and temperature for the SiC ladder. The laser displacement meter from Keyence Corp. has been used for the measurement. The survey system equipped with 2D motorized stages provided the 3D precision of about  $1 \mu\text{m}$  and was able to perform measurements for a ladder placed in a cryostat. Work is in progress to build and test further prototypes using the both types of foam with smaller fill factors.

## 5. Summary

A number of refined vertex algorithms are possible with a precise and thin detector at ILC. These algorithms are sensitive to the vertex detector design and can be used for its optimization, the most

compelling being the tagging of the heavy quark flavour based on vertex charge. The beampipe diameter, spatial resolution and the thickness of the detector are three most essential parameters for the optimization. Mechanically, ladders with thickness of 0.1%  $X_0$  seem achievable exploiting rigid foams based on silicon carbide or RVC.

## References

- [1] K. Abe *et al.*, *Nucl. Inst. Meth.* **A386** (1997) 46.
- [2] V. Chabaud *et al.*, *Nucl. Inst. Meth.* **A368** (1996) 314; D. Creanza *et al.*, *Nucl. Inst. Meth.* **A409** (1998) 157; P. P. Allport *et al.*, *Nucl. Inst. and Meth.* **A346** (1994) 476.
- [3] A. Sill for CDF collaboration, *Nucl. Inst. Meth.* **A447** (2000) 1; E. Kajfasz for D0 collaboration, *Nucl. Inst. Meth.* **A511** (2003) 16.
- [4] N. de Groot, *Nucl. Inst. Meth.* **A501** (2003) 229.
- [5] SLD collaboration, *Int J Mod Phys A* **16S1A** (2001) 274.
- [6] S. Hillert, C.J.S. Damerell on behalf of the LCFI Collaboration, Proceedings of the 2005 International Linear Collider Physics and Detector Workshop and 2nd ILC Accelerator Workshop (Snowmass 2005), SLAC-R-798 eConf: C0508141:ALCPG0101,(2005).
- [7] D. J. Jackson, *Nucl. Instr. Meth.* **A388** (1997) 247.
- [8] M. Battaglia, S. De Curtis, D. Dominici, S. Riemann, e-Print Archive: hep-ph/0112270.
- [9] G. A. Moortgat-Pick, Proceedings of the 2005 International Linear Collider Physics and Detector Workshop and 2nd ILC Accelerator Workshop (Snowmass 2005), eConf C0508141:ALCPG0306,2005, eConf C0508141:ALCPG0401,2005.
- [10] D. Auto, H. Baer, A. Belyaev, T. Krupovnickas, *Jour. High Ener. Phys.* 0410:066 (2004) 066.